Saudi Journal of Biological Sciences 29 (2022) 103296

Contents lists available at ScienceDirect

Saudi Journal of Biological Sciences

journal homepage: www.sciencedirect.com

Original article

Silver nanostructures prepared via novel green approach as an effective platform for biological and environmental applications

Pooja Rani [a,1], Bilal Ahmed [b,1], Jagpreet Singh [c,d,*], Jasmeen Kaur [e], Mohit Rawat [a,2], Navjot Kaur [f], Avtar Singh Matharu [g], Muneera AlKahtani [h], Eman A.H. Alhomaidi [h], Jintae Lee [b]

[a] Department of Nanotechnology, Sri Guru Granth Sahib World University, Fatehgarh Sahib 140406, Punjab, India
[b] School of Chemical Engineering, Yeungnam University, Republic of Korea
[c] Department of Chemical Engineering, Chandigarh University, Gharuan, Mohali 140413, India
[d] University Centre for Research and Development, Chandigarh University, Gharuan, Mohali 140413, India
[e] Department of Biotechnology, Sri Guru Granth Sahib World University, Fatehgarh Sahib 140406, Punjab, India
[f] Rayat Institute of Pharmacy, Railmajra, SBS Nagar, Punjab 144533, India
[g] Green Chemistry Centre of Excellence, Department of Chemistry, University of York, York YO10 5DD, UK
[h] Department of Biology, College of Sciences, Princess Nourah bint Abdulrahman University, P.O.Box 84428, Riyadh 11671, Saudi Arabia

ARTICLE INFO

Article history:
Received 24 January 2022
Revised 14 March 2022
Accepted 17 April 2022
Available online 22 April 2022

Keywords:
Silver nanostructures
Brassica oleracea
Glucose
Antimicrobial
Nitrophenol
Environmental

ABSTRACT

Silver nanoparticles play a significant role in biomedical sciences due to their unique properties allowing for their use as an effective sensing and remediation platform Herein, the green synthesis of silver nanostructures (Ag NSs), prepared via aqueous extract of waste *Brassica oleracea* leaves in the presence of silver nitrate solution (10^{-4} M), is reported. The Ag NSs are fully characterized and their efficacy with respect to 4-nitrophenol reduction, glucose sensing, and microbes is determined. Visually, the color of silver nitrate containing solution altered from colorless to yellowish, then reddish grey, confirming the formation of Ag NSs. HRTEM and SEAD studies revealed the Ag NSs to have different morphologies (triangular, rod-shaped, hexagonal, *etc.,* within a size range of 20–40 nm) with face-centered cubic (*fcc)* crystal structure. The Ag NSs possess high efficacy for nitrophenol reduction (<11 min and degradation efficiency of 98.2%), glucose sensing (LOD: 5.83 μM), and antimicrobial activity (*E. coli and B. subtilis* with clearance zones of 18.3 and 14 mm, respectively). Thus, the current study alludes towards the development of a cost-effective, sustainable, and efficient three-in-one platform for biomedical and environmental applications.

1. Introduction

In the past few decades, unprecedented interest and substantial research efforts have been made towards metallic nanoparticles, especially silver and gold, due to their exceptional chemical, biological, and physical properties (Bansal et al., 2007; Singh et al., 2020b; Tehri et al., 2022; Zhu et al., 2021). Specifically, silver nanoparticles (Ag NPs) gotten a lot of interest as antimicrobic agents in healthcare, cosmetics, food storage, textile coatings, and environmental remediation, such as, catalytic reduction of pollutant dyes (Baker et al., 2021; Dubey et al., 2010; Moradi et al., 2020; Rani et al., 2020; Singh et al., 2020a; Singh et al., 2018).

4-NP is widely used in pharmaceutical and agrochemical industries as a synthetic intermediate to many medicines, pesticides, and herbicides. However, the unregulated release of 4-NP when mixed with water is detrimental to freshwater bodies. 4-NP causes headaches, drowsiness, blood disorders, etc., and is a breakdown product from other pesticides, such as, parathion and fluoridifen. In 2002, Pal and Esumi first reported the ability of metal NPs to effectively reduce 4-NP to 4-AP in the existence of sodium borohydride. Thereafter, numerous researchers have used their study as a standard process to examine the catalytic potency of metal NPs, for example, Au NPs (Clarance et al., 2020; Khan et al., 2020), Ag NPs (Singh et al., 2017), Pd NPs (Nasrollahzadeh et al., 2015), Pt NPs

* Corresponding author at: Department of Chemical Engineering, University Centre for Research and Development, Chandigarh University, Gharuan, Mohali 140413, India.
E-mail addresses: jagpreet.e12147@cumail.in, jagpreetnano@gmail.com (J. Singh).
[1] These authors equally contributed to this work.
[2] Deceased author.

Peer review under responsibility of King Saud University.

Production and hosting by Elsevier

https://doi.org/10.1016/j.sjbs.2022.103296
1319-562X/

(Fahmy et al., 2020; Syed and Ahmad, 2012), and Ni NPs (Chaudhary et al., 2019).

Diabetes is a non-communicable disease and is identified as a global major health concern within the United Nations Sustainable Development Goals (SGD 3, Target 3.4). Amongst the most important clinical indicators of human health is blood glucose levels (Gao et al., 2017; Haleem et al., 2021; Huang et al., 2021). Glucose levels in the urine, on the other hand, are a good pre-screening signal for people with high blood sugar. The urine test is positive when the glucose concentration in the urine exceeds 500–1000 mg/L (Duc et al., 2018). A plethora of methods has been developed for glucose detection, such as spectrophotometry (Dong et al., 2021; Hwang et al., 2018; Journal, 2012), electrochemistry (Reghunath et al., 2021; Yoo and Lee, 2010; Yusan et al., 2018), chemiluminescence (Gao et al., 2021; Li et al., 2017), fluorometry (Han et al., 2019; Moschou et al., 2004; Yu et al., 2022), and surface-enhanced Raman spectroscopy (Cui et al., 2022; Sun, 2021). Despite these, the colorimetric method has attracted significant attention for detection due to its simplicity, lower cost, practicality, and portability (Li et al., 2013). These glucose sensors are dependent upon enzymes and chromogenic agents. The enzymatic oxidation of glucose produces gluconic acid and hydrogen peroxide. Although, natural enzymes have some limitations, for instance, the high cost of preparation, instability, purification, and storage.

Recently, several nanomaterials, namely: Fe_3O_4 (Ren et al., 2018; Sanaeifar et al., 2017), $ZnFe_2O_4$ (Shahnavaz et al., 2014; Su et al., 2012) magnetic nanoparticles, nitrogen-doped graphene quantum dots (Ji et al., 2016; Liu et al., 2020; Wu et al., 2020), C60 carboxy fullerenes (Dugan et al., 1997; Wei and Wang, 2008), graphite-like carbon nitrides (Wang et al., 2017), and CuS nanoparticles (Kim et al., 2017), have been reported to detect glucose using the colorimetric method.

Due to unique properties such as strong light absorption and scattering, high extinction coefficient (1×10^8 to 1×10^{10} M^{-1}-cm^{-1}), localised SPR, detection of metals rather than dyes, low cost-effectiveness, eco-friendliness, colorimetricity, and convenient bare detection, Ag NPs have a lot of potential in fundamental research and industrial applications (Syed and Ahmad, 2013; Syed et al., 2021). To date, various morphologies of silver nanostructures have been prepared (such as triangular, hexagonal, nanorods, nanoflowers, and nanowires). These morphologies offer interesting features (high surface area, high reactivity, and high adsorption potency in contrast to spherical ones, which play an influential role in many applications, including catalysis, antimicrobial activity. Thus, it is evident that AgNPs can be employed in diverse applications such as biomedical (e.g., glucose sensing and antimicrobial activity) and environmental (catalytic degradation of 4-NP).

Further, NPs have various synthesis methods, which involve biological, physical, and chemical processes. The use of expensive and dangerous chemicals, as well as the requirement of reactive reaction conditions, limits the applicability of these procedures. However, the green synthesis of NPs offers excellent advantages in contrast to previous ones, such as environmental friendliness, sustainability, and cost-effectiveness (Jadoun et al., 2021; Naikoo et al., 2021; Oves et al., 2022; Panda et al., 2020; Rana et al., 2020; Singh et al., 2019, 2018, 2017; Vanlalveni et al., 2021). To prepare NPs, these methods use a biological constituent, such as phytochemicals found in leaf extracts, as a reducing and capping agent.

In lieu of above discussion, herein, we report the green synthesis silver nanostructures (Ag NSs) using the aqueous extract from waste *Brassica oleracea* leaves as a three-in-one material for the transformation of 4-nitrophenol (4-NP) to 4-aminophenol, as a glucose sensor, and as an antimicrobial agent. The *Brassica oleracea* plant extract serves to reduce, stabilize and cap the *in-situ* formed Ag NSs. To the best of our knowledge, this is first study on the development of an efficient three-in-one platform prepared via waste leaves of plant for effective biomedical applications.

2. Experimental

2.1. Materials

Brassica Oleracea leaves were collected from the agriculture garden of SGGSWU campus, India, and thoroughly washed with distilled water. *Escherichia coli* and *Bacillus. subtilis* were supplied in-house by the Biotechnology Department, SGGSWU, campus. Merck provided 4-NP, sodium hydroxide (NaOH), sodium borohydride ($NaBH_4$), silver nitrate ($AgNO_3$), and, glucose oxidase (GOx). Sigma-Aldrich supplied the PBS (now known as Merck). Before use, all glassware carefully cleaned in aqua regia and wiped thoroughly double distilled water.

2.2. Formation of Ag NS

(see Fig. 1) A mixture of dried *Brassica oleracea* leaves (10 g) and DI water was boiled in a partially open beaker until it was reduced to one half of its original volume, filtered twice and the prepared *Brassica oleracea* extract was kept in a sealed container until it was needed again. An aliquot (1 mL) of the extract was poured to an aqueous mixture of $AgNO_3$ (50 mL, 1×10^{-4} M). The colour of the silver nitrate solution transformed from colourless to pale yellow to reddish-brown, indicating that Ag NSs had formed.

2.3. Glucose sensing

Ag NS solution (1000 μL) was added to a previously incubated (15 mins, water bath, 37 °C) mixture of the appropriate glucose solution (100 μL, 1 to 5 mM) in PBS buffer and GOx (100 μL; 2 mg/mL in 0.001 M PBS). The resultant mixtures were further incubated (water bath, 37 °C, 15 min) and, subsequently transferred into UV–Vis cuvettes and their UV–visible spectra recorded.

2.4. Catalytic potential: degradation of 4-NP

The appropriate aliquot of Ag NSs solution (5, 10, and 15 μL) was added to an aqueous mixture comprising 4-NP (5×10^{-3} M, 40 μL), $NaBH_4$ (300 μL, 2×10^{-1} M), and DI water (1.65 mL) contained within a UV-cuvette. UV–vis spectroscopy was used to monitor all this progress; besides this, every single min UV–vis spectra peaks were taken, awaiting significant changes. The catalytic experimentation was conducted in June 2021, with a solar flux of 632 W/m^2.

2.5. Antimicrobial activity

The "well-plate diffusion procedure" was employed to assess the antimicrobial potency of prepared Ag NSs. Bacterial cultures were cultivated in Petri plates containing Luria broth (LB) and incubated overnight. Wells were then knocked into the Luria broth plates. Ag NSs were then poured in the wells in various amounts (10, 20, 30, and 40 μL) and incubated overnight at 37 °C. On the following day, the antimicrobial property of AgNSs was monitored by visually checking for any zones of clearance.

2.6. Sample characterization

The optical examination of Ag NSs was carried out using a Shimadzu-UV 2600 UV–Vis spectrophotometer with a wavelength range of 200–800 nm, whereby, H_2O_2 (300 uL) was added, dropwise, the appropriate Ag NS solution (1 mL) contained in a UV-

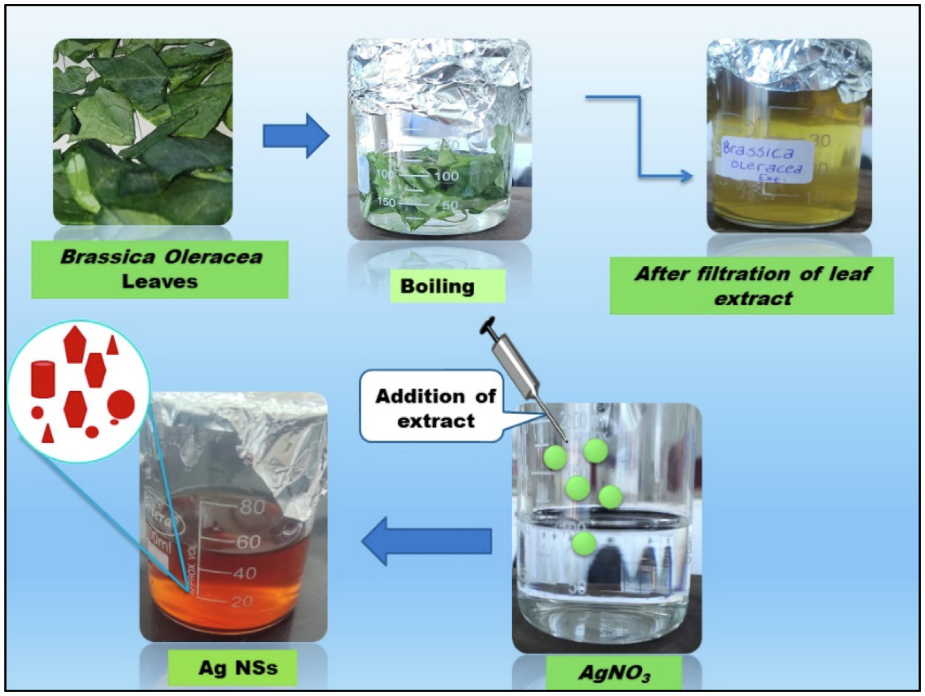

Fig. 1. Schematic showing the stepwise process for green synthesis of Ag NSs.

cuvette. An Alpha Fourier-transform infrared spectrophotometer was conducted to identify the phytochemicals contained in the extract and their interaction with Ag NSs. A (Malvern-ZEN-1690 instrument) was used to determine the average particle size (Z-average) and zeta potential (mV) of the as-prepared Ag NSs. The appropriate Ag NSs were dispersed in deionized water and sonicated for 10–15 min before insertion into the instrument High-resolution transmission electron microscopy (HR TEM; Jeol JEM-2100) to measure accurate particle size and morphological characteristics. Similarly, interplanar d-spacing and crystalline structure between the lattice planes were ascertained via selected area electron diffraction (SAED).

3. Results

3.1. Characterization of prepared Ag NSs

When the extract was added to the adequate silver nitrate solution, the colour changed from colourless to pale yellow to dark brown, indicating the growth of Ag NSs. The conversion of Ag^{+} to Ag^{0}, upon addition of *Brassica oleracea* extract, was evidenced through UV–Vis spectroscopy with advent of a surface plasmon resonance (SPR) band at 440–450 nm synonymous with Ag NSs as shown in Fig. 2(b). A strong absorption band at 442 nm was found after adding 1 mL, which correlates to the limited size distribution of synthesized particles. As a result, Ag NSs mediated by 1 mL extract were employed for further characterization and applications. FTIR spectroscopy was used to determine how much functionality was available on the AgNSs surface. The FTIR spectrum of Ag NSs as-prepared is shown in Fig. 2(c). Organic content on the surface of Ag NSs is indicated by high absorption peaks at 1024 (C-O, alcohol/ether stretch) 2921 cm^{-1} (C-H str.), 1521 cm^{-1} (C-C str.) 1737 cm^{-1} (C=O str.), and 3624 (O-H str.), (Huq, 2020). The organic matter functions as a cap on the AgNSs, preventing them from clumping together. The spikes observed at 704 and 644 cm^{-1} are caused by metal NPs stretching oscillations reacting with oxygen from the BO extract's hydroxyl group. (Khan et al., 2013; Shameli et al., 2012).

3.1.1. Particle size and zeta potential analysis

The average particle size of the as-prepared Ag NSs was determined by dynamic light scattering (DLS) to afford particles of 40.6 nm (Z-average) with a polydispersity index (PDI) of 0.225 as illustrated in Fig. 2(d). The zeta potential of prepared Ag NSs has been found to be –22.4 mV, demonstrating a -ve surface charge and stability.

3.1.2. HR-TEM analysis

HR-TEM was used to assess the size and structural configurations of the obtained Ag NSs (Fig. 3). The synthesized Ag NSs exhibited a variety of morphological types, such as, triangular, hexagonal, rod-shaped, and spherical with a size range from 20 to 40 nm as illustrated in Fig. 3a and b. The interatomic d-spacing across Ag NSs lattice fringes was measured at 0.24 nm (Fig. 3c), which corresponds to the (1 1 1) crystal plane. SAED analysis (Fig. 3d) was also used to determine interplanar spacing, which found around at 1.47, 2.44, 2.09, and 1.26, that correlates to the crystalline planes of (2 2 0), (1 1 1), (2 0 0), and (3 1 1) respectively. These findings are similar to the standard values for a crystal structure that is equivalent to the (fcc) crystal structure of the as-prepared Ag NSs (JCPDS no. 00–004-0783).

3.2. Applications of prepared Ag NSs

3.2.1. Catalytic activity

The catalytic potential of obtained Ag NSs with respect to the transformation of 4-NP to 4-AP, in the existence of $NaBH_4$, was inspected through UV–Vis spectroscopy (Fig. 4a-c). In the degradation of 4-NP, the characteristic, initial absorbance band of 4-NP undergoes a bathochromic (red) shift with hyperchromic effect as it converts into its corresponding intermediate nitrophenolate ion evidenced at 400 nm. Concomitantly, a new absorption band appeared at 297 nm, which increased in intensity, whilst the nitro-

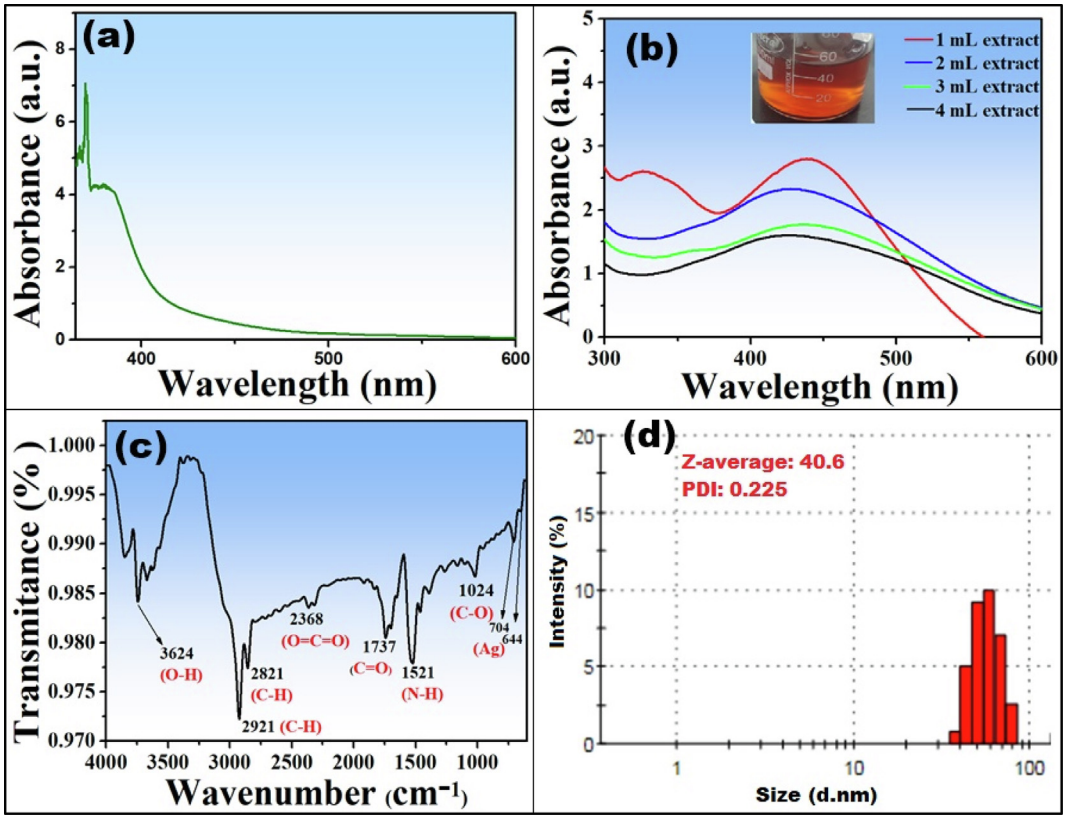

Fig. 2. Spectroscopic studies of Ag NSs: (a) UV–visible spectra of plant extract and (b) AgNSs with of differing volumes of extract, (c) FTIR spectrum (d) Particle size and distribution as determined by Zetasizer.

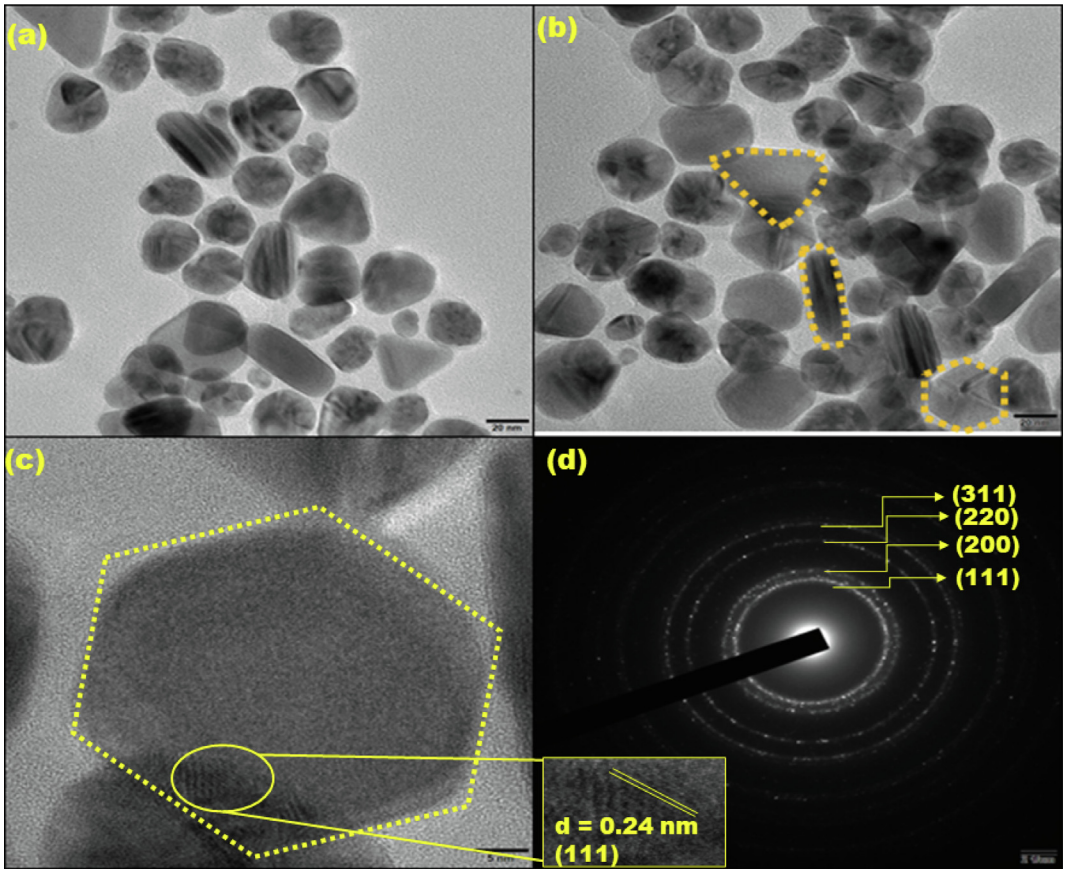

Fig. 3. Morphological characteristics of Ag NSs: (a-b) HR-TEM of Ag NSs at 20 nm scale bar, (c) Lattice fringes and d-spacing of Ag NSs at 5 nm scale bar and, (d) SAED pattern with corresponding crystal planes.

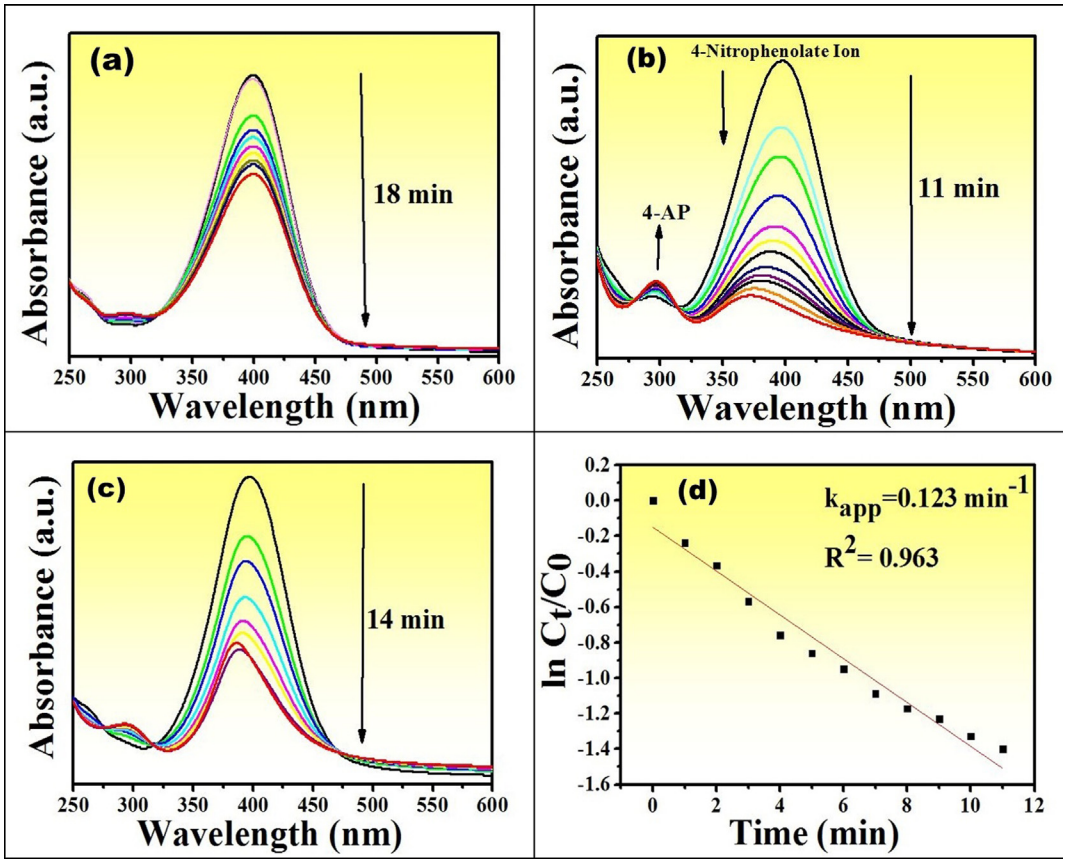

Fig. 4. 4-Nitrophenol reduction: UV–vis spectrum of catalytic potency of 4-NP degradation (a-c) using the different volume of Ag NSs (5, 10, and 15 µL) in the presence of 4-NP and $NaBH_4$ and (d) linear relationship between reaction time (min) and normalized concentration.

phenolate band decreased, as the reaction progressed (Fig. 4a-c). This reaction was investigated at the different proportion of Ag NSs (5, 10, and 15 µL). The best volume was deemed to be 10 µL of Ag NSs solution which gave complete degradation within 11 min (Fig. 4b). This could be because the reaction rate was reduced by a considerable amount of catalyst and capping agents (phytochemicals). As previously reported, increasing the volume of prepared extract and stabilising phytoconstituents delayed restructuration (redox interactions between reactant surfaces and catalyst) on the catalytic surface, resulting in a slower reaction rate (Rani et al., 2020). In the absenteeism of Ag NSs, the degradation of 4-NP was low, and the 4-nitrophenolate ion was not generated in the absence of sodium borohydride in a positive control (Figs. S1a and S1b).

A plot of the standardized concentration (C_t/C_0) vs time (Fig. 4d) yielded kinetic parameters, which were used to determine the apparent rate constant (K'_{app}) via a first-order rate law (equation (1)).

$$\ln\left(\frac{C_t}{C_0}\right) = -k'_{app}.t \quad (1)$$

Where C_0 and C_t are initial concentrations of the reactant i.e. 4-Nitrophenol at time t = 0 and final concentration at time t = t, respectively. With a correlation coefficient (R^2) of 0.963, the K'_{app} value was determined to be 0.123 min^{-1}. As a result, the catalytic study seems to obey a pseudo-first-order kinetic. Ag NSs are anticipated to lower the activation barrier among reactant and product owing to their large surface area and active surface locations (Zhao et al., 2015).

3.2.2. Glucose sensing

Glucose sensing can be readily monitored by observing changes in the surface plasmon resonance (SPR) band of Ag NSs (440–450 nm), which should decrease with a loss of color of the Ag NSs as glucose is oxidized as illustrated in Fig. 5a. The alteration in absorbance, ΔA, increased linearly with increasing the concentration of glucose. The limit of detection (LOD) has been measured to be 5.83 µM (Fig. 5b; gradient, 0.0857 and R^2, 0.966).

3.2.3. Antibacterial potency of Ag NSs

The antibacterial activities of AgNSs were explored using the Disc Diffusion method against two different bacterial strains (Fig. 6a-c). Diameter zones of inhibition were observed around wells treated with Ag NSs suspension, while negative control was showed by plates with $AgNO_3$, extract, and DI water, alone. The clearance zone grew in a linear relationship with the amount of Ag NSs applied.

3.3. Discussion

Regarding results of catalytic potential of Ag NSs, as per information available, a process for catalytic reduction of 4-NP is described in Fig. 7 for better understanding. Sodium borohydride was first added to the mixture, which caused 4-NP to deprotonate and change into a nitrophenolate ion. Despite this, highly efficient Ag NSs were utilized to reduce the viability of reaction by which kinetic energy barrier decreased between acceptor and donor molecules and convert nitrophenolate ions to 4-AP. Due to a considerable potential gradient among acceptor and donor molecules ((4-NP, BH_4^-: 0.7 V, 1.33 V) in the absence of Ag NSs, a strong acti-

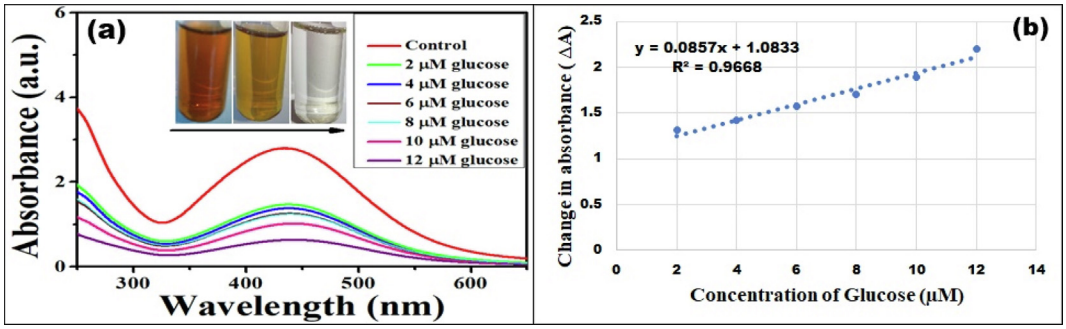

Fig. 5. Sensing characteristics of Ag NSs: (a) UV–vis absorption spectrum of Ag NSs *(inset: photographs of Ag NSs with glucose)*, and (b) kinetic study for LOD calculations.

vation energy barrier is formed. Silver-based nanocomposites were previously created using sophisticated chemical procedures like co-precipitation, hydrothermal polymerization, sol–gel, hydrolysis, and electrochemical synthesis. In the current work, however, a simple and naturally acceptable approach for reducing 4-NP was devised.

Lastly, we analysed the efficiency of Ag NPs as catalysts by comparing our findings to prior studies (Table 1). Based on the results of the analysis, Ag NPs based nanocomposites were developed for the removal of 4-NP from water. These procedures, on the other hand, are expensive and difficult, and they necessitate the use of quite sophisticated monitoring systems. As a result of present study, Ag NPs appear to be promising candidates for the catalytic reduction of nitro pollutants.

From a mechanistic point of view, the reaction of glucose with GOx produces H_2O_2 and gluconic acid. The resultant H_2O_2 oxidizes the Ag NSs (Ag^0) to silver ions (Ag^+) which led to a decline in the SPR band of Ag NSs and changing of color (equations (2) and (3)) Fig. 8.

$$\text{Glucose} + O_2 + H_2O_2 \rightarrow \text{D} - \text{Glucono} - 1,5 - \text{Lactone (gluconic acid)} + H_2O_2 \quad (2)$$

$$H_2O_2 + AgNSs \rightarrow Ag^+ ions \quad (3)$$

Moreover, the control experiment to validate the reaction between H_2O_2 and Ag NSs solutions, the absence of glucose) is illustrated in Fig. S2. It was pragmatic that leaching of Ag NSs with direct addition of H_2O_2 takes less time as compared to glucose. Thus, the described behavior provides a perspective for quantitative detection of glucose through observing the decline in SPR band and change in colour of Ag NSs.

The Ag NSs were found to possess higher antimicrobial activity towards gram-negative bacteria than the gram-positive bacteria. This difference may be interpreted from various emphasizing factors. First of all, differences in the architecture of cell walls of both types of bacteria, dictates the different functionality at the surface. Gram-positive (*Bacillus*) microbe have heavier cell walls that include peptidoglycan proteins, which makes them more resistant to Ag NSs than gram -ve bacteria. In addition, because the negative charge on gram-positive bacteria attracted more silver ions to the surface, the amount of Ag NSs that reached the plasma membrane was reduced.

Moreover, smaller NSs show high antimicrobial potential owing to the large surface area to interact than particles. The underlying rationale for Ag NSs' strong antibacterial activity, along with the conception of Ag+, is the creation of highly reactive oxygen species (ROS), that is regarded to become a key mechanism in apoptosis (Al-Sharqi et al., 2019; Lee et al., 2019). Previous works on antibacterial potential of biogenic Ag NSs demonstrated that these noble

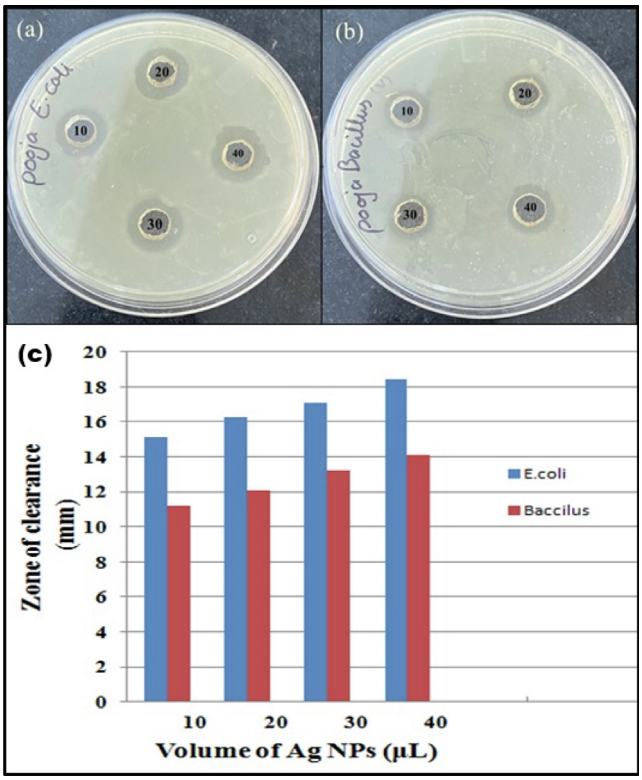

Fig. 6. Antibacterial activity of Ag NSs against (a) *E. coli* and, (b) *B. Subtilis*; (c) Histogram shows the zone of clearance w.r.t volume of Ag NSs.

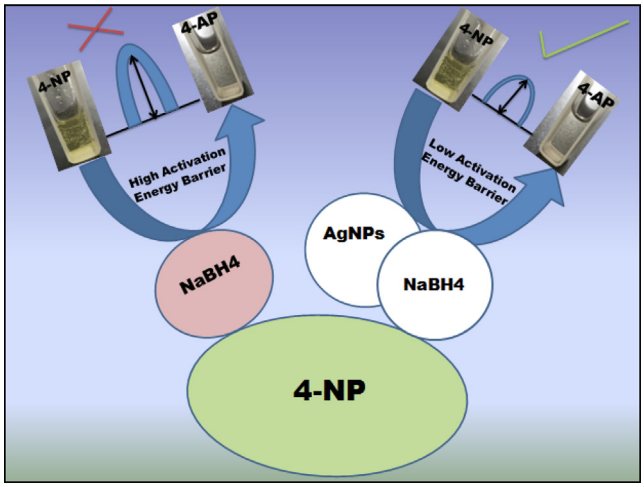

Fig. 7. Schematic represents the process of 4-NP reduction using Ag NSs.

Table 1
A comparison of Ag NPs and their composites' catalytic performance.

S/N	Catalyst	Preparation procedure	Catalyst loading (g)	Reaction time (min)	Ref.
1	Ag/PAN CFNs	Hydrothermal	0.01	70	(Gao et al., 2016)
2	Ag-P(NIPAM-co-AAm)	Precipitation polymerization	0.02	25	(Begum et al., 2016)
3	AgNP-enriched SiO_2	Green (seed mediated)	0.25	26	(Online and Lee, 2015)
4	CNC/CTAB/Ag	Hydrolysis	–	20	(An et al., 2016)
	Au, Ag NPs	Green	0.02	45	(Saha et al., 2010)
5	AgNPs	Biological	0.04	20	(Verma et al., 2016)
6	AgNPs/PD/ PANFP	Chemical	–	30	(Lu et al., 2017)
	Ag NPs by kollicoat	Chemical	0.05	60	(Sharma et al., 2016)
7	AgNPs/polymer	Chemical	0.2	30	(Xiao et al., 2012)
	Ag NPs	Biodegradable polymerization	0.03	12	(Safari et al., 2016)
9	Biogenic Ag NPs	Green	0.02	15	(Rani et al., 2020)
10	**Ag NSs**	**Green**	**0.02**	**11**	**Present study**

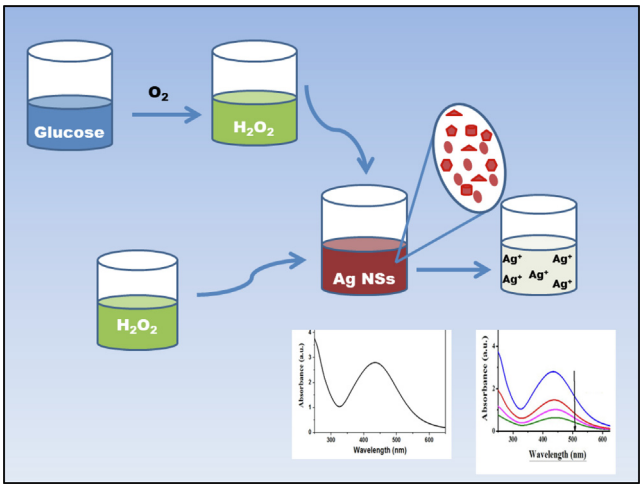

Fig. 8. Schematic represents the process of glucose sensing based on Ag NSs.

metal based NSs kill bacteria by a variety of mechanisms, including oxidative stress, Altered gene expression, protein degradation, and DNA damage, as well as disruption of cell transport membranes (Roy et al., 2019). Because of the inclusion of biomolecules, as-prepared Ag NSs are associated with more potent antibacterial action than available on the market/chemically approaches mediated NSs (Bagherzade et al., 2017).

4. Conclusions

In conclusion, diverse morphological Ag NSs were successfully prepared by utilizing waste leaves of *Brassica oleracea*. The synthesized Ag NSs showed excellent remediation potential based on the degradation of 4-nitrophenol and antimicrobial activity against gram +ve and gram −ve bacteria. Furthermore, the developed system also possesses remarkable colorimetric, as well as, spectrophotometric sensing of glucose and hydrogen peroxide, however, real sample study should be carried out in the future for industrial applications. Thus, this study encourages researchers to the development of waste into value-added products, which can be employed effectively in various biological and environmental applications.

Declaration of Competing Interest

The authors declare that they have no known competing financial interests or personal relationships that could have appeared to influence the work reported in this paper.

Acknowledgments

The authors gratefully acknowledge Chandigarh University, Mohali, Sri Guru Granth Sahib World University, Fatehgarh Sahib, Punjab (India) for research lab facilities. Authors are thankful to Department of Biotechnology, Sri Guru Granth Sahib World University, Fatehgarh Sahib and Sprint Testing Solutions, Mumbai for providing all necessary facilities carry out this research work. The authors extend their appreciation to Princess Nourah bint Abdulrahman University Researchers Supporting Project number (PNURSP2022R20), Princess Nourah bint Abdulrahman University, Riyadh, Saudi Arabia. This work was supported by National Research Foundation of Korea (NRF) grant funded by the Korean government (MSIT) (No. 2021R1G1A1094698).

Appendix A. Supplementary material

Supplementary data to this article can be found online at https://doi.org/10.1016/j.sjbs.2022.103296.

References

Al-Sharqi, A., Apun, K., Vincent, M., Kanakaraju, D., Bilung, L.M., 2019. Enhancement of the antibacterial efficiency of silver nanoparticles against gram-positive and gram-negative bacteria using blue laser light. Int. J. Photoenergy 2019, 1–12. https://doi.org/10.1155/2019/2528490.

An, X., Long, Y., Ni, Y., 2016. silver nanoparticle composite as a catalyst for reduction of. Carbohydr. Polym. https://doi.org/10.1016/j.carbpol.2016.08.099.

Bagherzade, G., Tavakoli, M.M., Namaei, M.H., 2017. Green synthesis of silver nanoparticles using aqueous extract of saffron (Crocus sativus L.) wastages and its antibacterial activity against six bacteria. Asian Pac. J. Trop. Biomed. 7 (3), 227–233. https://doi.org/10.1016/j.apjtb.2016.12.014.

Baker, A., Iram, S., Syed, A., Elgorban, A.M., Bahkali, A.H., Ahmad, K., Khan, M.S., Kim, J., 2021. Fruit derived potentially bioactive bioengineered silver nanoparticles. Int. J. Nanomed. 16, 7711–7726. https://doi.org/10.2147/IJN.S330763.

Bansal, V., Syed, A., Bhargava, S.K., Ahmad, A., Sastry, M., 2007. Zirconia enrichment in zircon sand by selective fungus-mediated bioleaching of silica. Langmuir 23 (9), 4993–4998. https://doi.org/10.1021/la062535x.

Begum, R., Farooqi, Z.H., Ahmed, E., Naseem, K., Ashraf, S., Sharif, A., Rehan, R., 2016. Catalytic reduction of 4 - nitrophenol using silver nanoparticles - engineered poly (N - isopropylacrylamide - co - acrylamide) hybrid microgels. 1–8. doi: 10.1002/aoc.3563

Chaudhary, J., Tailor, G., Yadav, B.L., Michael, O., 2019. Synthesis and biological function of Nickel and Copper nanoparticles. Heliyon 5 (6), e01878. https://doi.org/10.1016/j.heliyon.2019.e01878.

Clarance, P., Luvankar, B., Sales, J., Khusro, A., Agastian, P., Tack, J.-C., Al Khulaifi, M. M., AL-Shwaiman, H.A., Elgorban, A.M., Syed, A., Kim, H.-J., 2020. Green synthesis and characterization of gold nanoparticles using endophytic fungi Fusarium solani and its in-vitro anticancer and biomedical applications. Saudi J. Biol. Sci. 27 (2), 706–712. https://doi.org/10.1016/j.sjbs.2019.12.026.

Cui, X., Li, J., Li, Y., Liu, M., Qiao, J., Wang, D., Cao, H., He, W., Feng, Y., Yang, Z., 2022. Detection of glucose in diabetic tears by using gold nanoparticles and MXene composite surface-enhanced Raman scattering substrates. Spectrochim. Acta - Part A Mol. Biomol. Spectrosc. 266, 120432. https://doi.org/10.1016/j.saa.2021.120432.

Dong, Q., Ryu, H., Lei, Y., 2021. Metal oxide based non-enzymatic electrochemical sensors for glucose detection. Electrochim. Acta. 370, 137744. https://doi.org/10.1016/j.electacta.2021.137744.

Dubey, S.P., Lahtinen, M., Sillanpää, M., 2010. Green synthesis and characterizations of silver and gold nanoparticles using leaf extract of Rosa rugosa. Colloids Surfaces A Physicochem. Eng. Asp. 364 (1-3), 34–41. https://doi.org/10.1016/j.colsurfa.2010.04.023.

Duc, N., Nguyen, T. Van, Duc, A., Vinh, H., 2018. ORIGINAL ARTICLE A label-free colorimetric sensor based on silver nanoparticles directed to hydrogen peroxide and glucose. Arab. J. Chem. 11, 1134–1143. doi: 10.1016/j.arabjc.2017.12.035.

Dugan, L.L., Turetsky, D.M., Du, C., Lobner, D., Wheeler, M., Almli, C.R., Shen, C.K.F., Luh, T.Y., Choi, D.W., Lin, T.S., 1997. Carboxyfullerenes as neuroprotective agents. Proc. Natl. Acad. Sci. U. S. A. 94, 9434–9439. https://doi.org/10.1073/pnas.94.17.9434.

Fahmy, S.A., Preis, E., Bakowsky, U., Azzazy, H.M.E.S., 2020. Platinum nanoparticles: green synthesis and biomedical applications. Molecules 25, 1–17. https://doi.org/10.3390/molecules25214981.

Gao, Y., Wu, Y., Di, J., 2017. Colorimetric detection of glucose based on gold nanoparticles coupled with silver nanoparticles. SAA 173, 207–212. https://doi.org/10.1016/j.saa.2016.09.023.

Gao, Y., Huang, Y.u., Chen, J., Liu, Y., Xu, Y., Ning, X., 2021. A Novel luminescent "nanochip" as a tandem catalytic system for chemiluminescent detection of sweat glucose. Anal. Chem. 93 (30), 10593–10600. https://doi.org/10.1021/acs.analchem.1c01798.

Gao, S., Zhang, Z., Liu, K., Dong, B., 2016. Direct evidence of plasmonic enhancement on catalytic reduction of 4-nitrophenol over silver nanoparticles supported on flexible fibrous networks. Appl. Catal B, Environ. 188, 245–252. https://doi.org/10.1016/j.apcatb.2016.01.074.

Haleem, A., Javaid, M., Singh, R.P., Suman, R., Rab, S., 2021. Biosensors applications in medical field: a brief review. Sensors Int. 2, 100100. https://doi.org/10.1016/j.sintl.2021.100100.

Han, T., Zhu, S., Wang, S., Wang, B., Zhang, X., Wang, G., 2019. Fluorometric methods for determination of H2O2, glucose and cholesterol by using MnO2 nanosheets modified with 5-carboxyfluorescein. Microchim. Acta 186 (5). https://doi.org/10.1007/s00604-019-3381-1.

Huang, P., Xu, L., Xie, Y., 2021. Biomedical applications of electromagnetic detection: a brief review. Biosensors 11 (7), 225. https://doi.org/10.3390/bios11070225.

Huq, M.A., 2020. Green synthesis of silver nanoparticles using pseudoduganella eburnea MAHUQ-39 and their antimicrobial mechanisms investigation against drug resistant human pathogens. Int. J. Mol. Sci. 21 (4), 1510. https://doi.org/10.3390/ijms21041510.

Hwang, D.-W., Lee, S., Seo, M., Chung, T.D., 2018. Recent advances in electrochemical non-enzymatic glucose sensors – a review. Anal. Chim. Acta 1033, 1–34. https://doi.org/10.1016/j.aca.2018.05.051.

Jadoun, S., Arif, R., Jangid, N.K., Meena, R.K., 2021. Green synthesis of nanoparticles using plant extracts: a review. Environ. Chem. Lett. 19 (1), 355–374. https://doi.org/10.1007/s10311-020-01074-x.

Ji, H., Zhou, F., Gu, J., Shu, C., Xi, K., Jia, X., 2016. Nitrogen-doped carbon dots as a new substrate for sensitive glucose determination. Sensors (Switzerland) 16 (5), 630. https://doi.org/10.3390/s16050630.

Journal, T., 2012. A novel Spectrophotometric method for the trace analysis of glucose 4, 4731–4733.

Khan, M., Khan, M., Adil, S.F., Tahir, M.N., Tremel, W., Alkhathlan, H.Z., Al-Warthan, A., Siddiqui, M.R.H., 2013. Green synthesis of silver nanoparticles mediated by Pulicaria glutinosa extract. Int. J. Nanomed. 8, 1507–1516. https://doi.org/10.2147/IJN.S43309.

Khan, M., Al-Hamoud, K., Liaqat, Z., Shaik, M.R., Adil, S.F., Kuniyil, M., Alkhathlan, H. Z., Al-Warthan, A., Siddiqui, M.R.H., Mondeshki, M., Tremel, W., Khan, M., Tahir, M.N., 2020. Synthesis of au, ag, and au–ag bimetallic nanoparticles using pulicaria undulata extract and their catalytic activity for the reduction of 4-nitrophenol. Nanomaterials 10, 1–14. https://doi.org/10.3390/nano10091885.

Kim, W.B., Lee, S.H., Cho, M., Lee, Y., 2017. Facile and cost-effective CuS dendrite electrode for non-enzymatic glucose sensor. Sensors Actuators, B Chem. 249, 161–167. https://doi.org/10.1016/j.snb.2017.04.089.

Lee, B., Lee, M.J., Yun, S.J., Kim, K., Choi, I.H., Park, S., 2019. Silver nanoparticles induce reactive oxygen species-mediated cell cycle delay and synergistic cytotoxicity with 3-bromopyruvate in Candida albicans, but not in Saccharomyces cerevisiae. Int. J. Nanomedicine 14, 4801–4816. https://doi.org/10.2147/IJN.S205736.

Li, H., Liu, C., Wang, D., Zhang, C., 2017. Chemiluminescence cloth-based glucose test sensors (CCGTSs): a new class of chemiluminescence glucose sensors. Biosens. Bioelectron. 91, 268–275. https://doi.org/10.1016/j.bios.2016.12.004.

Li, R., Zhen, M., Guan, M., Chen, D., Zhang, G., Ge, J., Gong, P., Wang, C., Shu, C., 2013. A novel glucose colorimetric sensor based on intrinsic peroxidase-like activity of C60-carboxyfullerenes. Biosens. Bioelectron. 47, 502–507. https://doi.org/10.1016/j.bios.2013.03.057.

Liu, W., Jia, H., Zhang, J., Tang, J., Wang, J., Fang, D., 2020. Preparation of nitrogen-doped carbon quantum dots (NCQDs) and application for non-enzymatic detection of glucose. Microchem. J. 158, 105187. https://doi.org/10.1016/j.microc.2020.105187.

Lu, S., Yu, J., Cheng, Y., Wang, Q., Barras, A., Xu, W., Szunerits, S., Cornu, D., Boukherroub, R., 2017. Preparation of silver nanoparticles / polydopamine functionalized polyacrylonitrile fiber paper and its catalytic activity for the reduction 4-nitrophenol. Appl. Surf. Sci. 411, 163–169. https://doi.org/10.1016/j.apsusc.2017.03.120.

Moradi, M., Moussavi, G., Yaghmaeian, K., Yazdanbakhsh, A., Srivastava, V., Sillanpää, M., 2020. Synthesis of novel Ag-doped S-MgO nanosphere as an efficient UVA/LED-activated photocatalyst for non-radical oxidation of diclofenac: catalyst preparation and characterization and photocatalytic mechanistic evaluation. Appl. Catal. B Environ. 260. https://doi.org/10.1016/j.apcatb.2019.118128.

Moschou, E.A., Sharma, B.V., Deo, S.K., Daunert, S., 2004. Fluorescence glucose detection: advances toward the ideal in vivo biosensor. J. Fluoresc. 14 (5), 535–547. https://doi.org/10.1023/B:JOFL.0000039341.64999.83.

Naikoo, G.A., Mustaqeem, M., Hassan, I.U., Awan, T., Arshad, F., Salim, H., Qurashi, A., 2021. Bioinspired and green synthesis of nanoparticles from plant extracts with antiviral and antimicrobial properties: a critical review. J. Saudi Chem. Soc. 25 (9), 101304. https://doi.org/10.1016/j.jscs.2021.101304.

Nasrollahzadeh, M., Mohammad Sajadi, S., Rostami-Vartooni, A., Khalaj, M., 2015. Green synthesis of Pd/Fe3O4 nanoparticles using Euphorbia condylocarpa M. bieb root extract and their catalytic applications as magnetically recoverable and stable recyclable catalysts for the phosphine-free Sonogashira and Suzuki coupling reactions. J. Mol. Catal. A Chem. 396, 31–39. https://doi.org/10.1016/j.molcata.2014.09.029.

Online, V.A., Lee, K., 2015. RSC Adv. https://doi.org/10.1039/C5RA11892A.

Oves, M., Ahmar Rauf, M., Aslam, M., Qari, H.A., Sonbol, H., Ahmad, I., Sarwar Zaman, G., Saeed, M., 2022. Green synthesis of silver nanoparticles by Conocarpus Lancifolius plant extract and their antimicrobial and anticancer activities. Saudi J. Biol. Sci. 29 (1), 460–471. https://doi.org/10.1016/j.sjbs.2021.09.007.

Panda, M.K., Singh, Y.D., Behera, R.K., Dhal, N.K., 2020. Biosynthesis of nanoparticles and their potential application in food and agricultural sector. Nanotechnol. Life Sci., 213–225 https://doi.org/10.1007/978-3-030-39246-8_10.

Rana, A., Yadav, K., Jagadevan, S., 2020. A comprehensive review on green synthesis of nature-inspired metal nanoparticles: mechanism, application and toxicity. J. Clean. Prod. 272, 122880. https://doi.org/10.1016/j.jclepro.2020.122880.

Rani, P., Kumar, V., Singh, P.P., Matharu, A.S., Zhang, W., Kim, K.-H., Singh, J., Rawat, M., 2020. Highly stable AgNPs prepared via a novel green approach for catalytic and photocatalytic removal of biological and non-biological pollutants. Environ. Int. 143, 105924. https://doi.org/10.1016/j.envint.2020.105924.

Reghunath, R., devi, K., Singh, K.K., 2021. Recent advances in graphene based electrochemical glucose sensor. Nano-Struct. Nano-Objects 26, 100750. https://doi.org/10.1016/j.nanoso.2021.100750.

Ren, H., Ma, T., Zhao, J., Zhou, R., 2018. Vc-functionalized Fe3O4 nanocomposites as peroxidase-like mimetics for H2O2 and glucose sensing. Chem. Res. Chinese Univ. 34 (2), 260–268. https://doi.org/10.1007/s40242-018-7289-9.

Roy, A., Bulut, O., Some, S., Mandal, A.K., Yilmaz, M.D., 2019. Green synthesis of silver nanoparticles: biomolecule-nanoparticle organizations targeting antimicrobial activity. RSC Adv 9 (5), 2673–2702.

Safari, J., Enayati Najafabadi, A., Zarnegar, Z., Farkhonde Masoule, S., 2016. Catalytic performance in 4-nitrophenol reduction by Ag nanoparticles stabilized on biodegradable amphiphilic copolymers. Green Chem. Lett. Rev. 9 (1), 20–26. https://doi.org/10.1080/17518253.2015.1134680.

Saha, S., Pal, A., Kundu, S., Basu, S., Pal, T., 2010. Photochemical green synthesis of calcium-alginate-stabilized ag and au nanoparticles and their catalytic application to 4-nitrophenol reduction. Langmuir 26 (4), 2885–2893. https://doi.org/10.1021/la902950x.

Sanaeifar, N., Rabiee, M., Abdolrahim, M., Tahriri, M., Vashaee, D., Tayebi, L., 2017. A novel electrochemical biosensor based on Fe3O4 nanoparticles-polyvinyl alcohol composite for sensitive detection of glucose. Anal. Biochem. 519, 19–26. https://doi.org/10.1016/j.ab.2016.12.006.

Shahnavaz, Z., Lorestani, F., Alias, Y., Woi, P.M., 2014. Polypyrrole-ZnFe 2 O 4 magnetic nano-composite with core-shell structure for glucose sensing. Appl. Surf. Sci. 317, 622–629. https://doi.org/10.1016/j.apsusc.2014.08.194.

Shameli, K., Ahmad, M.B., Zamanian, A., Sangpour, P., Shabanzadeh, P., Abdollahi, Y., Zargar, M., 2012. Green biosynthesis of silver nanoparticles using Curcuma longa tuber powder. Int. J. Nanomed. 7, 5603–5610. https://doi.org/10.2147/IJN.S36786.

Sharma, M., Mishra, A., Kumar, V., Basu, S., 2016. Green synthesis of silver nanoparticles with exceptional colloidal stability and its catalytic activity toward nitrophenol reduction. NANO 11 (04), 1650046. https://doi.org/10.1142/S1793292016500466.

Singh, J., Dutta, T., Kim, K.-H., Rawat, M., Samddar, P., Kumar, P., 2018. "Green" synthesis of metals and their oxide nanoparticles: applications for environmental remediation. J. Nanobiotechnol. 16 (1). https://doi.org/10.1186/s12951-018-0408-4.

Singh, J., Kukkar, P., Sammi, H., Rawat, M., Singh, G., Kukkar, D., 2017. Enhanced catalytic reduction of 4-nitrophenol and congo red dye *By* silver nanoparticles prepared from *Azadirachta indica* leaf extract under direct sunlight exposure. Part. Sci. Technol., 1–10.

Singh, J., Kaur, N., Singh, J., Kumar, S., Singh, P., Al-Rashed, S., Kaur, H., Rawat, M., 2020. An efficient and viable photodegradation of a textile Reactive yellow-86 dye under direct sunlight by multi-structured Fe2O3 encapsulated with phytochemicals of R. Indica. J. Mater. Sci. Mater. Electron. doi: 10.1007/S10854-020-04636-5.

Singh, S.P., Ansari, M.I., Pandey, B., Srivastava, J.K., Yadav, T.P., Rani, H., Parveen, A., Mala, J., Singh, A.K., 2020. Recent trends and advancement toward phyto-mediated fabrication of noble metallic nanomaterials: focus on silver, gold, platinum, and palladium, in: Nanotechnology in the Life Sciences, pp. 87–105. doi: 10.1007/978-3-030-34544-0_6

Singh, J., Kumar, V., Kim, K.-H., Rawat, M., 2019. Biogenic synthesis of copper oxide nanoparticles using plant extract and its prodigious potential for photocatalytic

degradation of dyes. Environ. Res. 177, 108569. https://doi.org/10.1016/j.envres.2019.108569.
Su, L., Feng, J., Zhou, X., Ren, C., Li, H., Chen, X., 2012. Colorimetric detection of urine glucose based ZnFe2O4 magnetic nanoparticles. Anal. Chem. 84 (13), 5753–5758. https://doi.org/10.1021/ac300939z.
Sun, X., 2021. Glucose detection through surface-enhanced Raman spectroscopy: a review. Anal. Chim. Acta., 339226 https://doi.org/10.1016/j.aca.2021.339226.
Syed, A., Ahmad, A., 2012. Extracellular biosynthesis of platinum nanoparticles using the fungus Fusarium oxysporum. Colloids Surf. B Biointerfaces 97, 27–31. https://doi.org/10.1016/j.colsurfb.2012.03.026.
Syed, A., Ahmad, A., 2013. Extracellular biosynthesis of CdTe quantum dots by the fungus Fusarium oxysporum and their anti-bacterial activity. Spectrochim. Acta - Part A Mol. Biomol. Spectrosc. 106, 41–47. https://doi.org/10.1016/j.saa.2013.01.002.
Syed, A., Al Saedi, M.H., Bahkali, A.H., Elgorban, A.M., Kharat, M., Pai, K., Ghodake, G., Ahmad, A., 2021. Biological synthesis of α-Ag2S composite nanoparticles using the fungus Humicola sp. and its biomedical applications. J. Drug Deliv Sci. Technol. 66, 102770. https://doi.org/10.1016/j.jddst.2021.102770.
Tehri, N., Vashishth, A., Gahlaut, A., Hooda, V., 2022. Biosynthesis, antimicrobial spectra and applications of silver nanoparticles: current progress and future prospects. Inorg. Nano-Metal Chem. doi: 10.1080/24701556.2020.1862212.
Vanlalveni, C., Lallianrawna, S., Biswas, A., Selvaraj, M., Changmai, B., Rokhum, S.L., 2021. Green synthesis of silver nanoparticles using plant extracts and their antimicrobial activities: a review of recent literature. RSC Adv. 11 (5), 2804–2837.
Verma, A.D., Jain, N., Singha, S.K., Quraishi, M.A., Sinha, I., 2016. Green synthesis and catalytic application of curcumin stabilized silver nanoparticles. 128, 1871–1878. doi: 10.1007/s12039-016-1189-7.
Wang, A., Wang, C., Fu, L., Wong-Ng, W., Lan, Y., 2017. Recent advances of graphitic carbon nitride-based structures and applications in catalyst, sensing, imaging, and leds. Nano-Micro Lett. 9, 1–21. https://doi.org/10.1007/s40820-017-0148-2.
Wei, H., Wang, E., 2008. Colorimetric detection of urine glucose based ZnFe2O4 magnetic nanoparticles. Anal. Chem. 80, 2250–2254. https://doi.org/10.1021/ac702203f.
Wu, H., Yan, Y., Huang, Q., Liang, G., Qiu, F., Ye, Z., Liu, D., 2020. A simple, cost-effective and selective analysis of glucose via electrochemical impedance sensing based on copper and nitrogen co-doped carbon quantum dots. New J. Chem. 44 (29), 12723–12728.
Xiao, S., Xu, W., Ma, H., Fang, X.u., 2012. Size-tunable Ag nanoparticles immobilized in electrospun nanofibers: synthesis, characterization, and application for catalytic reduction of 4-nitrophenol. RSC Adv. 2 (1), 319–327.
Yoo, E.-H., Lee, S.-Y., 2010. Glucose biosensors: an overview of use in clinical practice. Sensors 10 (5), 4558–4576. https://doi.org/10.3390/s100504558.
Yu, Q., Jiang, J., Chen, Z., Han, C., Zhang, X., Yang, S., Zhou, P., Deng, T., Yu, C., 2022. A multilevel fluorometric biosensor based on boric acid embedded in carbon dots to detect intracellular and serum glucose. Sensors Actuators B Chem. 350, 130898. https://doi.org/10.1016/j.snb.2021.130898.
Yusan, S., Rahman, M.M., Mohamad, N., Arrif, T.M., Latif, A.Z.A., Mohd Aznan, M.A., Wan Nik, W.S.B., 2018. Development of an amperometric glucose biosensor based on the immobilization of glucose oxidase on the Se-MCM-41 mesoporous composite. J. Anal. Methods Chem. 2018, 1–8. https://doi.org/10.1155/2018/2687341.
Zhao, P., Feng, X., Huang, D., Yang, G., Astruc, D., 2015. Basic concepts and recent advances in nitrophenol reduction by gold- and other transition metal nanoparticles. Coord. Chem. Rev. 287, 114–136. https://doi.org/10.1016/j.ccr.2015.01.002.
Zhu, X., Blanco, E., Bhatti, M., Borrion, A., 2021. Impact of metallic nanoparticles on anaerobic digestion: a systematic review. Sci. Total Environ. 757, 143747. https://doi.org/10.1016/j.scitotenv.2020.143747.